nature geoscience

PROGRESS ARTICLE

PUBLISHED ONLINE: 25 JULY 2016 | DOI: 10.1038/NGEO2757

An abyssal carbonate compensation depth overshoot in the aftermath of the Palaeocene–Eocene Thermal Maximum

Donald E. Penman[1]*, Sandra Kirtland Turner[2], Philip F. Sexton[3], Richard D. Norris[4], Alexander J. Dickson[5], Slah Boulila[6,7], Andy Ridgwell[2], Richard E. Zeebe[8], James C. Zachos[9], Adele Cameron[3], Thomas Westerhold[10] and Ursula Röhl[10]

During the Palaeocene–Eocene Thermal Maximum (PETM) about 56 million years ago, thousands of petagrams of carbon were released into the atmosphere and ocean in just a few thousand years, followed by gradual sequestration over approximately 200,000 years. If silicate weathering is one of the key negative feedbacks that removed this carbon, a period of seawater calcium carbonate saturation greater than pre-event levels would be expected during the event's recovery phase. In marine sediments, this should be recorded as a temporary deepening of the depth below which no calcite is preserved — the calcite compensation depth (CCD). Previous and new sedimentary records from sites that were above the pre-PETM CCD show enhanced carbonate accumulation following the PETM. A new record from an abyssal site in the North Atlantic that lay below the pre-PETM CCD shows a period of carbonate preservation beginning about 70,000 years after the onset of the PETM, providing the first direct evidence for an over-deepening of the CCD. This record confirms an overshoot in ocean carbonate saturation during the PETM recovery. Simulations with two earth system models support scenarios for the PETM that involve a large initial carbon release followed by prolonged low-level emissions, consistent with the timing of CCD deepening in our record. Our findings indicate that sequestration of these carbon emissions was most likely the result of both globally enhanced calcite burial above the CCD and, at least in the North Atlantic, an over-deepening of the CCD.

The PETM represents one of the largest and most abrupt greenhouse warming events in Earth's history. Marine and terrestrial records document a global >2.5‰ negative carbon isotope excursion (CIE; refs 1–3) coincident with global mean surface ocean warming of >4 °C (ref. 4) and geochemical and sedimentological evidence for ocean acidification[5,6]. Collectively, these lines of evidence suggest a rapid (10^3–10^4 years) and massive (~3,000–10,000 PgC) release of ^{13}C-depleted carbon into the ocean–atmosphere system[7–9]. The PETM thus offers the opportunity to examine the response and recovery of the global carbon cycle and seawater carbonate chemistry to an ancient CO_2 release similar in magnitude to ongoing anthropogenic fossil fuel combustion[10].

Current understanding of long-term carbon cycle processes predicts that a rapid carbon injection should cause a short-term (0 to tens of thousands of years (kyr)) period of ocean acidification featuring reduced seawater carbonate saturation (Ω), followed by a longer-term (10–100 kyr) period of carbonate oversaturation due to elevated rates of terrestrial silicate weathering (see Box 1). This carbonate saturation overshoot manifests itself in several carbon cycle model simulations of the PETM[9,11] as an over-deepening of the CCD relative to its pre-event depth. Yet no records exist from abyssal sites below the pre-PETM CCD with which to detect possible CCD over-deepening. Sedimentary records from above the CCD (Southern Ocean Site 690 (refs 12–15) at ~1,900m palaeodepth, and South Atlantic Site 1263 (refs 6,14,15) at ~1500m palaeodepth and Site 1266 (refs 6,16) at ~2,500m palaeodepth) show increases in the carbonate ($CaCO_3$) content and accumulation rate during and after the PETM recovery[13–15]. These supra-CCD records are consistent with increased carbonate burial prompted by weathering feedbacks during the PETM recovery and provide important constraints, because the long-term requirement to balance the elevated weathering flux only requires carbonate burial to increase globally (not necessarily at greater depths). It is thus theoretically possible to accommodate such an elevated rate of global carbonate burial without substantial deepening of the CCD[17]. Nonetheless, some models[9–11] predict that a testable facet of the recovery process from a massive carbon cycle perturbation involves an over-deepening of the CCD, and the location of these sites above the pre-PETM CCD means that they cannot directly test for this predicted CCD over-deepening. Direct observational evidence from sites that are sufficiently deep to test for a post-PETM CCD overshoot has thus far remained elusive.

Here we present the lithology, $CaCO_3$ content and carbon isotope ($\delta^{13}C$) records from recently recovered sediment cores in the North Atlantic[18] (IODP Site U1403, PETM palaeodepth ~4,374 m and Site U1409, palaeodepth ~2,913 m) that provide important constraints on the evolution of the CCD through the PETM, including the

[1]Department of Geology & Geophysics, Yale University, New Haven, Connecticut 05611, USA. [2]Department of Earth Science, University of California, Riverside, California 92521, USA. [3]Department of Environment, Earth and Ecosystems, The Open University, Milton Keynes MK7 6AA, UK. [4]Scripps Institute of Oceanography, La Jolla, California 92093, USA. [5]Department of Earth Sciences, University of Oxford, Oxford OX1 3AN, UK. [6]Université Paris VI, CNRS UMR 7193, Institut des Sciences de la Terre-Paris (ISTeP), case 117, 4 place Jussieu, 75252 Paris Cedex 05, France. [7]ASD, IMCCE-CNRS UMR 8028, Observatoire de Paris, UPMC, 77 Avenue Denfert-Rochereau, 75014 Paris, France. [8]Department of Oceanography, University of Hawaii at Manoa, Honolulu, Hawaii 96822, USA. [9]Department of Earth & Planetary Science, University of California, Santa Cruz, California 95064, USA. [10]MARUM—Center for Marine Environmental Sciences, University of Bremen, D-28359 Bremen, Germany. *e-mail: donald.penman@yale.edu

Box 1 | The ocean's two-phase response to rapid carbon injection.

Current understanding of long-term carbon cycle processes suggests that a large-scale injection of carbon into the ocean–atmosphere system should induce a two-phase response in ocean carbonate saturation. Initially, the rapid invasion of CO_2 into the ocean lowers pH and Ω in tandem[5,37,40], resulting in dissolution of both newly deposited and pre-existing carbonate sediments[6]. The result is a dramatic reduction in $CaCO_3$ burial in marine sediments globally and, in places, evidence for a shoaling of the CCD[6,24,41].

A second phase of the carbonate saturation and burial response arises from the elevated atmospheric CO_2 concentration and increased global temperatures that are thought to drive an increase in the rate of terrestrial $CaCO_3$ and silicate rock chemical weathering[42,43], which can be generalized by:

$$CaCO_3 + CO_2 + H_2O \rightarrow Ca^{2+} + 2HCO_3^- \quad (1)$$

$$CaSiO_3 + 2CO_2 + 3H_2O \rightarrow Ca^{2+} + 2HCO_3^- + H_4SiO_4 \quad (2)$$

Accelerating these reactions increases the delivery of Ca^{2+} (and thus the total alkalinity) and dissolved inorganic carbon (DIC) to the oceans, elevating Ω. An intensification of continental weathering during the PETM is supported by a pronounced increase in the $^{187}Os/^{188}Os$ ratio of seawater[44,45] and an increase in kaolinite in marine sediments[46]. However, although the silicate weathering rate responds quickly to increased temperature or CO_2 concentration, the rate of CO_2 drawdown from global weathering (~0.1 PgC yr^{-1}; ref. 40) is small in comparison to estimates of initial carbon release (thousands of PgC)[7–9], meaning that this feedback should take >10^4 years to gradually overcome the undersaturation associated with the initial acidification phase[11,47,48]. On longer timescales (>100 kyr)[48], this increased weathering-derived flux of total alkalinity and DIC to the oceans must be balanced by carbonate production and burial to balance the ocean's alkalinity budget:

$$Ca^{2+} + 2HCO_3^- \rightarrow CaCO_3 + CO_2 + H_2O \quad (3)$$

The long-term balance of carbonate weathering with carbonate burial has no permanent effect on the ocean's total alkalinity or DIC budgets (equation (1) is simply the reverse of equation (3)). However, the long-term balance of silicate weathering (equation (2)) with carbonate burial (equation (3)) gives rise to a net consumption of CO_2 that is buried as $CaCO_3$ sediments — the long-term fate of carbon released during the PETM.

The assumption that net CO_2 consumption via elevated silicate weathering and carbonate burial (equations (2) and (3)) is responsive to perturbations in climate forms the basis of a proposed long-term negative (stabilizing) feedback on climate, hypothesized to have been important in maintaining a habitable climate throughout Earth's history[42,43] and specifically during the PETM recovery[11]. One way that global carbonate burial could respond to a changing weathering flux is through fluctuations of the global seafloor area of carbonate-free sediments (that is, the CCD). In other words, during the initial acidification phase, carbonate undersaturation leads to a reduced $CaCO_3$ sink and a short-term shoaling of the CCD, whereas on longer timescales (>100 kyr), faster weathering rates lead to carbonate oversaturation and increased carbonate burial, which might be reflected in an over-deepening of the CCD[10,11,49]. The interval of excess (compared with pre-PETM) $CaCO_3$ burial primarily reflects the removal of carbon that was released at the onset of the PETM by enhanced silicate weathering, together with the quantity of $CaCO_3$ dissolved during the initial carbonate undersaturation phase and additional terrestrial weathering of carbonate rocks under warmer temperatures (both of which will be some function of CO_2 release). The characteristics of any post-PETM CCD overshoot hence potentially hold key information regarding the magnitude of the carbon release and the processes involved in the recovery from an abrupt perturbation of the carbon cycle.

first evidence for CCD over-deepening during the PETM recovery. To explore the broader implications of these records for PETM carbon emission scenarios, we present new carbon release experiments using two carbon cycle models — LOSCAR (refs 9,19) and cGENIE (refs 20,21) — and discuss the uncertainties in the representation of geological carbon cycling in current models.

New records from the North Atlantic

At Site U1409 the PETM CIE occurs in an interval of variously silicified sediments (siliceous claystones, siliceous limestones and cherts) at 178.9–179.2 m composite depth (m.c.d.; Fig. 1a), contrasting with the nannofossil chalk that characterizes much of the Palaeogene at this site[18]. Although is it likely to be condensed due to difficulty recovering such a varied lithology, the carbon isotopic composition of bulk carbonate (denoted $\delta^{13}C_{carb}$) record bears the typical[15] PETM CIE pattern of an abrupt decrease (here of ~2‰) followed by a plateau of low values and then a gradual recovery (Fig. 1). Bulk $\delta^{13}C_{carb}$ over the PETM CIE interval sampled a heterogeneous mixture of lithologies (clay, carbonate-rich burrows within that clay and siliceous sediments), with all three revealing significantly lower $\delta^{13}C$ values during the CIE than before the event. The integrity of the bulk $\delta^{13}C_{carb}$ record is also supported by the close structural similarity between it and the equivalent bulk $\delta^{13}C_{carb}$ records from the Southern Ocean (Site 690) and Walvis Ridge (Site 1263) (Figs 1 and 2a). The $\delta^{13}C$ record from Site U1409 for benthic foraminifera is discontinuous owing to silicification across the onset and initial recovery, but minimum values within the CIE show a large (~3‰) excursion, similar to that seen in benthic records from the Southern Ocean[22] and South Atlantic[23]. Below the CIE, the carbonate content is between 60–70 wt%, decreasing to a minimum of ~40 wt% at the CIE onset before rebounding to ~70% following the CIE. This pattern is similar to other pelagic PETM sections[24] and implies that the local CCD was always deeper than the palaeodepth of Site U1409, whereas the decrease in the carbonate content during the PETM can be interpreted as a transient decrease in Ω, consistent with shoaling of the CCD. The absence of near-zero wt% $CaCO_3$ sediments at Site U1409 contrasts with records from the South Atlantic Ocean[6] where cores even shallower than Site U1409 are barren of carbonate within the CIE. Although this observation could imply that CCD shoaling in the North Atlantic was less dramatic than in the South Atlantic. Hiatuses in sedimentation, bioturbation by burrowing or the incomplete recovery of this silicified interval could also have obscured or resulted in the loss of the interval that contains the lowest wt% $CaCO_3$ values. Regardless, the carbonate content and accumulation rate at Site U1409 were higher during the PETM recovery than before the event, similar to other sites at mid-ocean depths or shallower[6,12–14,16], thus providing support for elevated Ω and increased carbonate burial above the CCD during the recovery phase.

The lower-abyssal Site U1403 features a prominent transition (over ~5 cm) from carbonate-poor (<0.5 wt%) claystone in the Upper Palaeocene (extending from the Palaeocene/Eocene boundary to at least ~61 million years ago (Ma); ref. 18) to carbonate-bearing (~20–30 wt%) nannofossil claystones in the Lower Eocene (Fig. 1b). This carbonate-rich interval contains calcareous nannofossils of biostratigraphic zone NP9b, including the PETM excursion

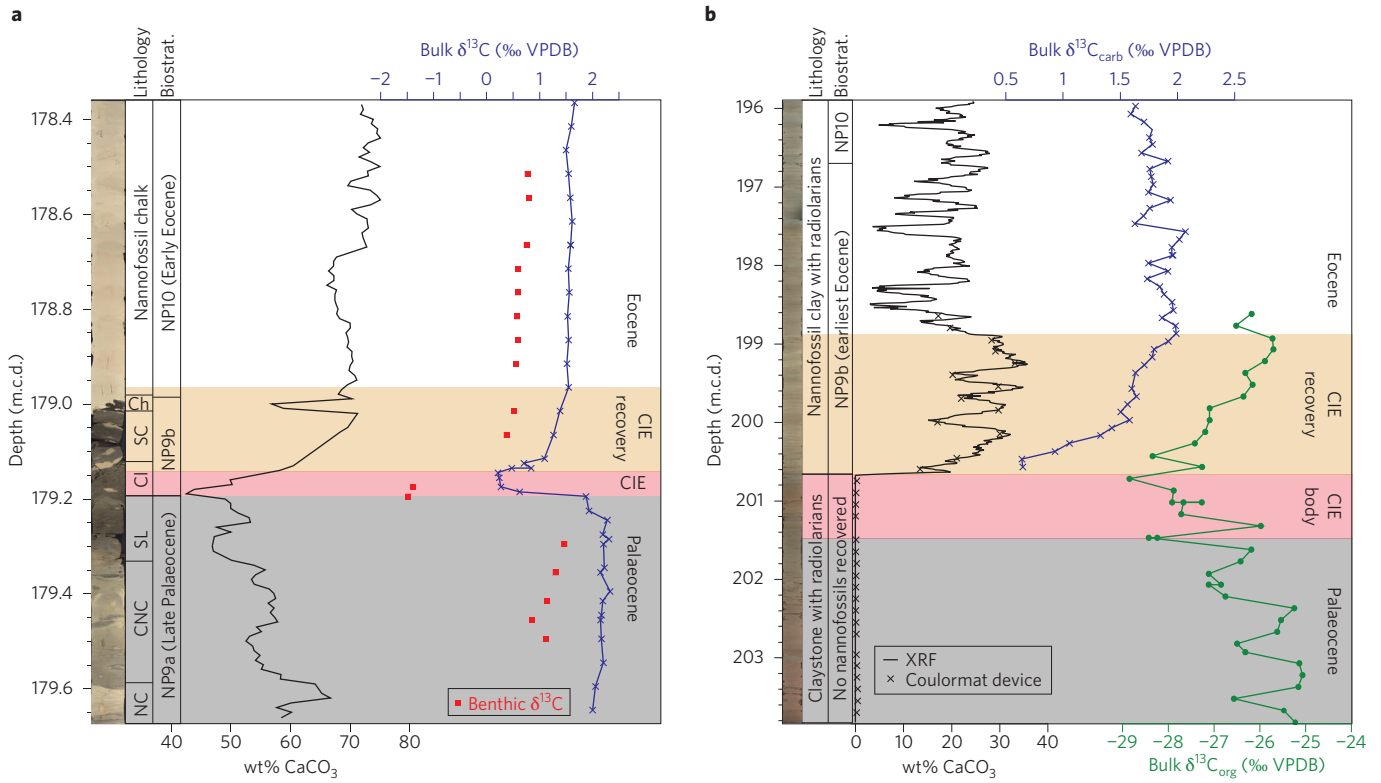

Figure 1 | Lithology and $\delta^{13}C$ over the PETM. a,**b**, Site U1409 (**a**) and Site U1403 (**b**). Each panel shows a core photo (left; Site U1403 vertically compressed), a lithologic description, the calcareous nannofossil biostratigraphy (biostrat.), the wt% $CaCO_3$ estimated by X-ray fluorescence (XRF) scanning data, and bulk $\delta^{13}C_{carb}$. Ch, chert; Cl, claystone; CNC, clayey nannofossil chalk; NC, nannofossil chalk; SC, siliceous claystone; SL, siliceous limestone. VPDB, Vienna Pee Dee Belemnite, the standard against which $\delta^{13}C$ was measured. Bulk $\delta^{13}C_{org}$ and wt% $CaCO_3$ measured with a Coulormat device are also shown for Site U1403, and benthic foraminifer *Nuttalides truempyi* $\delta^{13}C$ is shown for Site U1409. The heterogeneous mixture of clay- and carbonate-rich facies within the CIE at Site U1409 is interpreted as carbonate-rich burrows within clay-rich sediments, with both recording low (<0.5‰) bulk $\delta^{13}C$. The PETM phase nomenclature is from ref. 15.

taxa *Discoaster araneus* and *Rhomboaster* spp. (ref. 18). Bulk $\delta^{13}C_{org}$ (organic carbon) reveals a negative CIE between 200.7 and 201.5 m.c.d. that is superimposed on comparatively high-amplitude orbital-scale variability in the Late Palaeocene. The $\delta^{13}C_{carb}$ record necessarily begins at the onset of carbonate sedimentation, with low values of ~0.6‰, followed by a gradual 1.4‰ increase over the next ~1.6 m — parallel to the recovery in $\delta^{13}C_{org}$. Given the simultaneous trends towards higher values in both $\delta^{13}C_{carb}$ and $\delta^{13}C_{org}$ within zone NP9b, this $\delta^{13}C$ increase can be unambiguously assigned to the PETM CIE recovery. The magnitude of the $\delta^{13}C_{carb}$ increase (1.4‰) is close to the full amplitude of the PETM CIE recovery observed in bulk carbonates globally[15] and at Site U1409 (Fig. 2a), so we confidently assign the onset of carbonate sedimentation at Site U1403 to early in the PETM recovery phase.

We construct age models by correlating the $\delta^{13}C_{carb}$ records with a compilation of bulk and fine-fraction $\delta^{13}C_{carb}$ in an orbitally calibrated age model[15] (Fig. 2a,c). On the basis of several PETM sites, this model produces a shorter duration of the PETM CIE than extraterrestrial ^{3}He-based estimates[12,16], so durations here may represent minima. On this timescale, carbonate sedimentation begins at Site U1403 ~70 kyr after the PETM onset and is followed by a period of elevated (20–40) wt% $CaCO_3$ that persists for a further ~150 kyr. Fluctuations from 5–25 wt% $CaCO_3$ continue throughout the Lower Eocene. Although the onset of the CIE at Site U1403 (as defined by the noise in the $\delta^{13}C_{org}$ record) introduces some uncertainty around the placement of the Palaeocene/Eocene boundary, this does not affect the relative timing of the initial appearance of carbonate at this lower-abyssal site, which is unambiguously assigned to the PETM recovery interval based on $\delta^{13}C_{carb}$ and the occurrence of PETM excursion-interval calcareous nannofossils.

The pattern of carbonate sedimentation at Site U1403 (carbonate-barren in the Palaeocene with carbonate appearing during the PETM recovery) has not previously been observed in sediments that span the PETM. The absence of carbonate in the Upper Palaeocene and into the earliest Eocene indicates that the CCD lay shallower than Site U1403 before the PETM and through the onset and main part of the CIE. The start of carbonate sedimentation ~70 kyr after the onset of the PETM indicates that the CCD over-deepened to below the ~4,400 m lower-abyssal palaeowater depth of Site U1403 during the early phase of the PETM recovery — direct evidence for a post-PETM CCD overshoot. The ~150 kyr period of elevated carbonate deposition at Site U1403 represents the main phase of the CCD over-deepening, and is coeval with enhanced carbonate accumulation and preservation at shallower palaeodepths documented here at Site U1409 and elsewhere[6,13,14,16] (Fig. 2d). These observations strongly implicate an elevated whole-ocean Ω as the cause of enhanced carbonate burial at all water depths from the North Atlantic to the Southern Ocean.

CCD overshoot explored with carbon cycle models

To explore the implications of a CCD overshoot and its timing, and the CCD over-deepening at U1403 in particular, we tested a variety of PETM carbon emission scenarios using the LOSCAR and cGENIE models. Rather than carry out an extensive sweep of all of the plausible combinations of the size and duration of the carbon release, our scenarios are based on ref. 9 (characterized by an initial C input ($\delta^{13}C$ = −50‰) of 3,000 PgC over 5 kyr, followed by 1,480 PgC over 50 kyr), which was originally developed to match records of carbonate dissolution (particularly in the South Atlantic[6]). However, we explored a number of variations on this basic emissions trajectory (Supplementary Figs 4–15) such as doubling the total mass of carbon

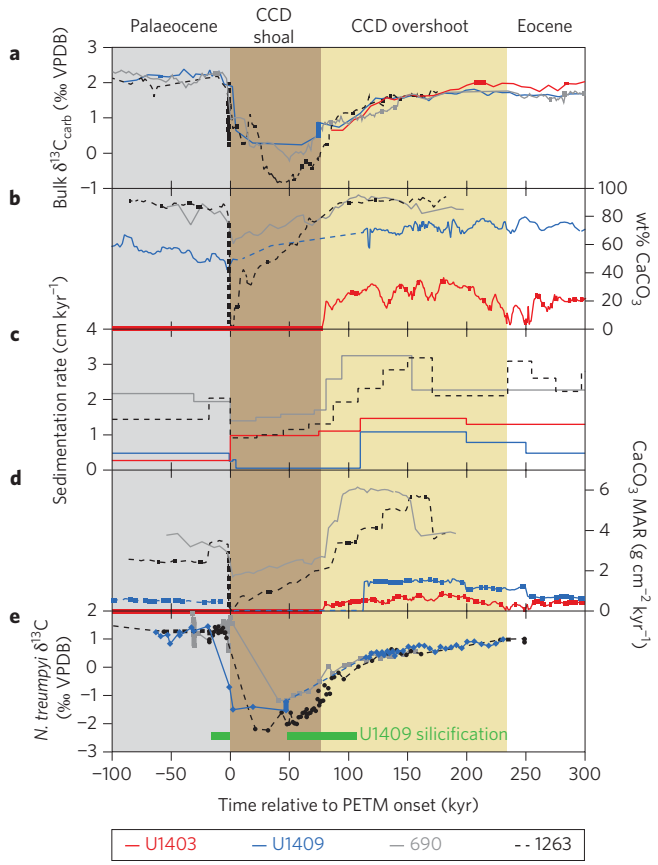

Figure 2 | Age models and PETM isotopic and sedimentological records from new and previous sites. a, Bulk $\delta^{13}C_{carb}$ records from sites 690 (ref. 13), 1263 (ref. 15), U1403 and U1409 plotted on the age model used in this study. **b**, Weight per cent $CaCO_3$ of sites U1403 and U1409 (this study), 690 (ref. 13) and 1263 (ref. 6). **c**, Linear sedimentation rates used in the age model constructed by this study for sites U1403 and U1409 and sites 690 and 1263 from ref. 15. **d**, Carbonate mass accumulation rate (MAR)calculated from the dry bulk density and data in **b** and **c**. **e**, Comparison of benthic foraminifer $\delta^{13}C$ from sites 1263 (ref. 23), 690 (ref. 22) and U1409 demonstrating a small and constant North–South Atlantic aging gradient during the CCD overshoot. The green bars indicate silicified intervals at Site U1409 that precluded the measurement of benthic foraminifers. In **b**,**d**,**e** the silicified interval of U1409 is marked with a dashed line to reflect potential hiatuses or incomplete recovery, which may have resulted in an incomplete $\%CaCO_3$ record (see text).

with half of the isotopic composition ($\delta^{13}C$ = –25‰). To isolate the response of the carbonate burial dynamics from circulation effects that might diverge in the two models, we ran cGENIE with radiative forcing (and thus ocean circulation) fixed. For direct comparison with cGENIE (Fig. 3) we also omitted the prescribed circulation changes of ref. 9 in LOSCAR. We tracked the evolution of the global wt% $CaCO_3$ preserved in sediments and simulated the expected marine sediment record in modelled 'cores' at North Atlantic depths that approximate sites U1409 and U1403.

The configurations used here for both LOSCAR and cGENIE include a CO_2-dependent silicate weathering feedback (see Methods). Both models simulate a global CCD and wt% $CaCO_3$ overshoot that occurs between 20 and 45 kyr after the onset of carbon emissions and peaks between 65 and 97 kyr after the onset, depending on the emissions schedule and model (Fig. 3 and Supplementary Fig. 3)[9,11]. The carbonate overshoot begins earlier when the carbon pulse occurs over a shorter interval (Supplementary Figs 6 and 12). The long delay (~70 kyr) in the onset of carbonate sedimentation at Site U1403 that we infer from our age model is hence difficult to reconcile with only a short 'spike' of carbon released at the onset of the PETM. The delay is better explained by a sustained release of carbon lasting many tens of thousands of years after an initial spike (Fig. 3 and Supplementary Fig. 1), consistent with the conclusions of ref. 9 and ref. 5. Such sustained carbon release might arise as a feedback response to initial warming[25,26] or represent prolonged North Atlantic volcanism. Our experiments also demonstrate that the timing of the overshoot is not particularly sensitive to the mass of carbon released — doubling the mass of carbon results in a delay of <2 kyr in the timing of the overshoot (for example, Supplementary Fig. 4 versus Supplementary Fig. 5).

Although both models generate a whole-ocean carbonate burial overshoot during the recovery interval, the spatial distribution of $CaCO_3$ content in the sediments shows differences both between the models and in comparison with sites U1403 and U1409 (Fig. 3). Because LOSCAR has much coarser spatial resolution (for example, it represents the deep Atlantic as a single box), regional patterns need to be interpreted with greater caution. Nevertheless, LOSCAR generates a deep (4,500 m water depth) wt% $CaCO_3$ overshoot comparable to that seen at Site U1403, but in shallow sediments (3,000 m) it generates a larger wt%$CaCO_3$ decrease (to near-zero) and a smaller overshoot than seen at Site U1409. In contrast, cGENIE closely matches the record for Site U1409, but at 5,000 m, sediments overshoot their pre-event wt%$CaCO_3$ levels by only ~1%, in conflict with the Site U1403 record. It seems that in response to enhanced weathering-driven saturation states, LOSCAR accommodates greater global carbonate burial with higher wt% $CaCO_3$ in deep sediments (an over-deepening of the CCD), whereas cGENIE accommodates greater global carbonate burial predominantly within and above the lysocline. Observational evidence (in the form of new and previous records of carbonate accumulation rates) suggest that in the real world (at least in the case of the PETM), both of these processes may operate.

The differences between the models' predictions for the locus of intensified carbonate burial result from how they represent sedimentary processes. In cGENIE, the respiration of organic carbon in sediments reduces the porewater saturation state and dissolves $CaCO_3$, even in shallow sediments well above the carbonate saturation horizon. Because of this, those shallow sediments have greater potential to accommodate an increase in $CaCO_3$ content in response to a higher bottom-water saturation state such as that seen in the aftermath of the PETM. cGENIE thus balances an enhanced weathering flux via increased carbonate burial, mostly in shallow sediments within and above the lysocline[17]. Conversely, wt% $CaCO_3$ in sediments above the lysocline in LOSCAR is set by the ratio of clay to $CaCO_3$ in the sediment rain (81% $CaCO_3$ in the present configuration)[19], so when saturation state increases those shallow sediments cannot accommodate higher $CaCO_3$ contents (they are already at a maximum). Hence, LOSCAR balances an increase in the weathering flux via increased carbonate burial within the lysocline and below the (pre-event) CCD.

A notable feature of the carbonate record at Site U1403 is that following the main phase of the CCD over-deepening (where the highest carbonate contents are found), the wt% $CaCO_3$ does not return to 0% (its pre-event level) before the next major hyperthermal (Eocene Thermal Maximum 2, ~2,000 kyr later[18]) (Figs 1 and 2). Hence, the North Atlantic CCD did not return to its pre-PETM state. Two possible explanations exist for this observation. First, the negative feedbacks on carbonate undersaturation could have been very slow to re-establish equilibrium. This is unlikely, given that all of the other records of environmental and carbon-cycle perturbations during the PETM (such as temperature[4], pH[5] and the CIE[15]) recovered within hundreds of thousands of years, not millions. Second, the carbon cycle might have transitioned to a new equilibrium state that featured a deeper CCD. Several mechanisms may help to explain a deeper post-PETM equilibrium CCD in the North Atlantic. Importantly, the evolution of the PETM CCD may have been superimposed

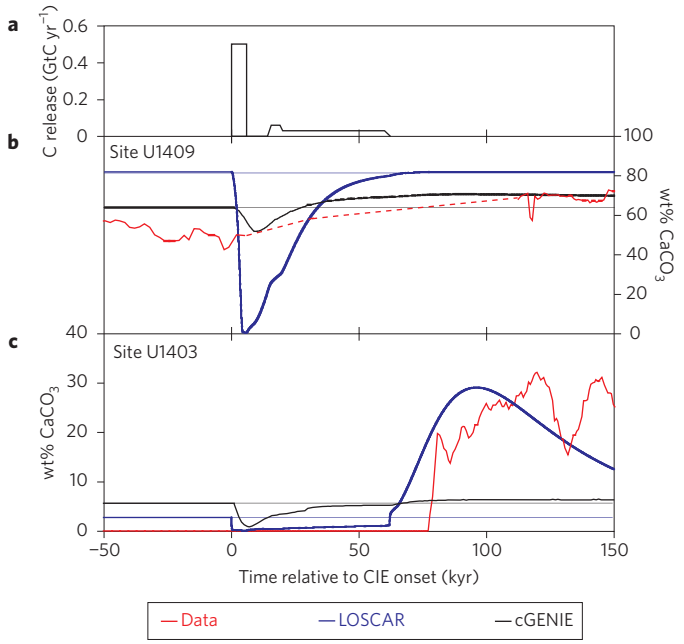

Figure 3 | Comparison of LOSCAR and cGENIE carbon release experiments. Radiative forcing (and thus circulation) were fixed in cGENIE, and no circulation changes were implemented in LOSCAR. **a**, Emissions scenario, using the same parameters as ref. 9. **b**, Modelled 3,000 m sediment wt% $CaCO_3$ compared with data from Site U1409. The silicified interval of U1409 is marked with a dashed line to reflect potential hiatuses or incomplete recovery, which may have resulted in an incomplete %$CaCO_3$ record (see text). **c**, Modelled 4,500 m (LOSCAR) and 5,000 m (cGENIE) sediment wt% $CaCO_3$ compared with data from Site U1403. In **b** and **c** the thin, opaque traces mark pre-event wt% $CaCO_3$ for both models.

on a long-term (multimillion year) deepening trend in the global CCD[27–30]. Increasing atmospheric CO_2 concentration on multimillion year timescales across the Late Palaeocene–Early Eocene from greater volcanic CO_2 release or an imbalance between terrestrial C_{org} oxidation and marine C_{org} burial could have strengthened weathering rates — thus increasing seawater carbonate saturation and driving a gradual CCD deepening from ~58 to ~52 Ma — independently of the PETM[27]. Indeed, LOSCAR simulations of the carbon release superimposed on gradual long-term CCD deepening (Supplementary Fig. 2) agree well with observations from Site U1403, including the persistence of the overshoot.

Changing ocean circulation or regional carbonate export across the PETM might have also affected the regional North Atlantic CCD (that is, the observed CCD over-deepening was not necessarily global). Weakened overturning originating in the North Atlantic during the acidification phase followed by strengthened overturning during the oversaturation phase could have produced the initial large CCD shoal documented at Walvis Ridge[6] (South Atlantic) and the later CCD over-deepening at Site U1403 (North Atlantic). If such circulation changes persisted for several million years, they could have produced a persistently deeper post-PETM North Atlantic CCD. Spatial benthic $\delta^{13}C$ gradients can shed light on circulation changes[22], because the accumulation of respired C_{org} reduces the $\delta^{13}C$ of deep water DIC as it ages. Owing to its location in the lower abyss, Site U1403 is unfortunately nearly barren of benthic foraminifera throughout the PETM and its recovery. However, Site U1409 benthic $\delta^{13}C$ values overlap with those of the South Atlantic[23] and Southern Ocean[22] during intervals immediately before the PETM and during the later stages of the recovery — including the time interval (>110 kyr after the event) during which Site U1403 documents a CCD overshoot (Fig. 2). Benthic gradients between the South and North Atlantic therefore do not show any evidence for large-scale changes in Atlantic overturning circulation during the PETM recovery that could have contributed to a localized CCD over-deepening.

Other processes could also have contributed to CCD over-deepening during the PETM recovery, specifically those processes that could have removed carbon from the ocean–atmosphere and increased seawater pH and Ω (in a sense, the opposite of the PETM acidification phase) and hence influenced the CCD. In particular, studies have suggested[31] that the pace of the CIE recovery, which is complete within ~150 kyr (refs 12,16), is too rapid to be explained by enhanced weathering and carbonate burial alone. Instead, the preferential removal of ^{12}C via enhanced burial of organic carbon has been proposed to explain the CIE recovery timing[31]. This is consistent with evidence of increased marine productivity during the PETM from elevated biogenic barium accumulation rates[32,33] and coccolith Sr/Ca ratios[34]. Our model experiments focus on the long-term inorganic carbon cycle and silicate weathering and hence cannot exclude a role for enhanced burial of organic carbon.

Our finding of a post-PETM CCD overshoot in the North Atlantic constitutes the first evidence for post-PETM variations in carbonate burial from sediments deeper than the pre-PETM CCD. It thus represents an important constraint on the vertical extent of the response of the CCD to carbon release during the PETM, and consequently on the processes responsible for restoring the carbon cycle to a steady state. It is tempting to use this information to directly calculate the mass of carbon released during the PETM, because the excess carbonate burial should scale with the mass of carbon released. However, we recognize that one site does not fully constrain the global extent of the overshoot, nor its absolute magnitude. Further limits on the extent of CCD over-deepening from even deeper sites and other ocean basins are therefore an essential target for future scientific drilling. Uncertainty in the strength of the silicate weathering feedback[35] (Supplementary Fig. 2) — as well as the potential influences of the initial carbon cycle conditions, circulation changes, C_{org} burial and changing clay flux — also preclude an explicit calculation of the total carbon release[10]. Indeed, the differing responses of the two different global carbon cycle models we have tested against the observations underscore the lack of consensus on how the marine carbonate carbon sink responds in detail (and particularly in the depth distribution of $CaCO_3$ burial) to perturbation. Multiple combinations of the mass and rate of the carbon release, the strength of the weathering feedback and C_{org} burial rates are consistent with the new observations described here. Our findings nevertheless provide an important constraint on how carbon was sequestered in the aftermath of the PETM, an event that continues to guide our understanding of Earth system processes and feedbacks during large-scale perturbations to the carbon cycle.

Methods

Methods and any associated references are available in the online version of the paper.

Received 1 April 2016; accepted 7 June 2016;
published online 25 July 2016

References

1. Koch, P. L., Zachos, J. C. & Gingerich, P. D. Correlation between isotope records in marine and continental carbon reservoirs near the Palaeocene/Eocene boundary. *Nature* **358,** 319–322 (1992).
2. Kennett, J. P. & Stott, L. D. Abrupt deep-sea warming, palaeoceanographic changes and benthic extinctions at the end of the Palaeocene. *Nature* **353,** 225–229 (1991).
3. McInerney, F. A. & Wing, S. The Paleocene–Eocene Thermal Maximum: a perturbation of carbon cycle, climate, and biosphere with implications for the future. *Annu. Rev. Earth Planet. Sci.* **39,** 489–516 (2011).
4. Dunkley-Jones, T. *et al.* Climate model and proxy data constraints on ocean warming across the Paleocene–Eocene Thermal Maximum. *Earth Sci. Rev.* **125,** 123–145 (2013).

5. Penman, D. E., Hönisch, B., Zeebe, R. E., Thomas, E. & Zachos, J. C. Rapid and sustained surface ocean acidification during the Paleocene–Eocene Thermal Maximum. *Paleoceanography* **29,** 357–369 (2014).
6. Zachos, J. C. *et al.* Rapid acidification of the ocean during the Paleocene–Eocene Thermal Maximum. *Science* **308,** 1611–1615 (2005).
7. Dickens, G. R., Oneil, J. R., Rea, D. K. & Owen, R. M. Dissociation of oceanic methane hydrate as a cause of the carbon isotope excursion at the end of the Paleocene. *Paleoceanography* **10,** 965–971 (1995).
8. Panchuk, K., Ridgwell, A. & Kump, L. R. Sedimentary response to Paleocene–Eocene Thermal Maximum carbon release: a model-data comparison. *Geology* **36,** 315–318 (2008).
9. Zeebe, R. E., Zachos, J. C. & Dickens, G. R. Carbon dioxide forcing alone insufficient to explain Palaeocene–Eocene Thermal Maximum warming. *Nature Geosci.* **2,** 576–580 (2009).
10. Zeebe, R. & Zachos, J. Long-term legacy of massive carbon input to the Earth system: Anthropocene versus Eocene. *Phil. Trans. R. Soc. A* **371,** 1–22 (2012).
11. Dickens, G. R., Castillo, M. M. & Walker, J. C. G. A blast of gas in the latest Paleocene: simulating first-order effects of massive dissociation of oceanic methane hydrate. *Geology* **25,** 259–262 (1997).
12. Farley, K. A. & Eltgroth, S. F. An alternative age model for the Paleocene–Eocene thermal maximum using extraterrestrial ^{3}He. *Earth Planet. Sci. Lett.* **208,** 135–148 (2003).
13. Kelly, D. C., Zachos, J. C., Bralower, T. J. & Schellenberg, S. A. Enhanced terrestrial weathering/runoff and surface ocean carbonate production during the recovery stages of the Paleocene–Eocene thermal maximum. *Paleoceanography* **20,** PA4023 (2005).
14. Kelly, D. C., Nielsen, T. M. J., McCarren, H. K., Zachos, J. C. & Rohl, U. Spatiotemporal patterns of carbonate sedimentation in the South Atlantic: implications for carbon cycling during the Paleocene–Eocene thermal maximum. *Palaeogeogr. Palaeoclimatol. Palaeoecol.* **293,** 30–40 (2010).
15. Röhl, U., Westerhold, T., Bralower, T. J. & Zachos, J. C. On the duration of the Paleocene–Eocene thermal maximum (PETM). *Geochem. Geophys. Geosyst.* **8,** Q12002 (2007).
16. Murphy, B. H., Farley, K. A. & Zachos, J. C. An extraterrestrial He-3-based timescale for the Paleocene–Eocene thermal maximum (PETM) from Walvis Ridge, IODP Site 1266. *Geochim. Cosmochim. Acta* **74,** 5098–5108 (2010).
17. Greene, S. *et al.* Rethinking controls on the long-term cenozoic carbonate compensation depth: case studies across Late Paleocene–Early Eocene warming and Late Eocene–Early Oligocene cooling. Abstr. PP41C-1407 (American Geophysical Union, Fall Meeting, 2014).
18. Norris, R. D., Wilson, P. A., Blum, P. & the Expedition 342 Scientists. *Proc. IODP* Vol. 342 (IODP, 2012).
19. Zeebe, R. LOSCAR: Long-term Ocean-atmosphere-Sediment CArbon cycle reservoir model v2.0.4. *Geosci. Model Dev.* **5,** 149–166 (2012).
20. Ridgwell, A. & Hargreaves, J. Regulation of atmospheric CO_2 by deep-sea sediments in an Earth system model. *Glob. Biogeochem. Cycles* **21,** GB2008 (2007).
21. Ridgwell, A. Interpreting transient carbonate compensation depth changes by marine sediment core modeling. *Paleoceanography* **22,** PA4102 (2007).
22. Nunes, F. & Norris, R. D. Abrupt reversal in ocean overturning during the Palaeocene/Eocene warm period. *Nature* **439,** 60–63 (2006).
23. McCarren, H., Thomas, E., Hasegawa, T., Röhl, U. & Zachos, J. C. Depth dependency of the Paleocene-Eocene carbon isotope excursion: paired benthic and terrestrial biomarker records (Ocean Drilling Program Leg 208, Walvis Ridge). *Geochem. Geophys. Geosyst.* **9,** Q10008 (2008).
24. Zeebe, R. E. & Zachos, J. C. Reversed deep-sea carbonate ion basin gradient during Paleocene–Eocene thermal maximum. *Paleoceanography* **22,** PA3201 (2007).
25. Zeebe, R. E. What caused the long duration of the Paleocene–Eocene Thermal Maximum? *Paleoceanography* **26,** 1–13 (2013).
26. Bowen, G. J. Up in smoke: A role for organic carbon feedbacks in Paleogene hyperthermals. *Glob. Planet. Change* **109,** 18–29 (2013).
27. Komar, N., Zeebe, R. & Dickens, G. Understanding long-term carbon cycle trends: the late Paleocene through the early Eocene. *Paleoceanography* **28,** 650–662 (2013).
28. Leon-Rodriguez, L. & Dickens, G. R. Constraints on ocean acidification associated with rapid and massive carbon injections: the early Paleogene record at ocean drilling program site 1215, equatorial Pacific Ocean. *Palaeogeogr. Palaeoclimatol. Palaeoecol.* **298,** 409–420 (2010).
29. Hancock, H. J., Dickens, G. R., Thomas, E. & Blake, K. L. Reappraisal of early Paleogene CCD curves: foraminiferal assemblages and stable carbon isotopes across the carbonate facies of Perth Abyssal Plain. *Int. J. Earth Sci.* **96,** 925–946 (2007).
30. Slotnick, B. S. *et al.* Early Paleogene variations in the calcite compensation depth: new constraints using old borehole sediments from across Ninetyeast Ridge, central Indian Ocean. *Clim. Past* **11,** 473–493 (2015).
31. Bowen, G. J. & Zachos, J. C. Rapid carbon sequestration at the termination of the Palaeocene–Eocene Thermal Maximum. *Nature Geosci.* **3,** 866–869 (2010).
32. Bains, S., Norris, R. D., Corfield, R. M. & Faul, K. L. Termination of global warmth at the Palaeocene/Eocene boundary through productivity feedback. *Nature* **407,** 171–174 (2000).
33. Ma, Z. *et al.* Carbon sequestration during the Palaeocene–Eocene Thermal Maximum by an efficient biological pump. *Nature Geosci.* **7,** 382–388 (2014).
34. Stoll, H. M. & Bains, S. Coccolith Sr/Ca records of productivity during the Paleocene–Eocene thermal maximum from the Weddell Sea. *Paleoceanography* **18,** 1049 (2003).
35. Uchikawa, J. & Zeebe, R. E. Influence of terrestrial weathering on ocean acidification and the next glacial inception. *Geophys. Res. Lett.* **35,** L23608 (2008).
36. Ridgwell, A. Application of sediment core modelling to interpreting the glacial–interglacial record of Southern Ocean silica cycling. *Clim. Past* **3,** 387–396 (2007).
37. Ridgwell, A. & Schmidt, D. N. Past constraints on the vulnerability of marine calcifiers to massive carbon dioxide release. *Nature Geosci.* **3,** 196–200 (2010).
38. Colbourn, G., Ridgwell, A. & Lenton, T. The Rock Geochemical Model (RokGeM) v0. 9. *Geosci. Model Dev.* **6,** 1543–1573 (2013).
39. Walker, J. C. G. & Kasting, J. F. Effects of fuel and forest conservation on future levels of atmospheric carbon dioxide. *Palaeogeogr. Palaeoclimatol. Palaeoecol.* **97,** 151–189 (1992).
40. Hönisch, B. *et al.* The geological record of ocean acidification. *Science* **335,** 1058–1063 (2012).
41. Sluijs, A., Zachos, J. C. & Zeebe, R. E. Constraints on hyperthermals. *Nature Geosci.* **5,** 231–231 (2012).
42. Walker, J. C. G., Hays, P. B. & Kasting, J. F. A Negative feedback mechanism for the long-term stabilization of Earths surface-temperature. *J. Geophys. Res.* **86,** 9776–9782 (1981).
43. Berner, R. A., Lasaga, A. C. & Garrels, R. M. The carbonate-silicate geochemical cycle and its effects on atmospheric carbon dioxide over the past 100 million years. *Am. J. Sci.* **283,** 641–683 (1983).
44. Dickson, A. J. *et al.* Evidence for weathering and volcanism during the PETM from Arctic Ocean and Peri-Tethys osmium isotope records. *Palaeogeogr. Palaeoclimatol. Palaeoecol.* **438,** 300–307 (2015).
45. Ravizza, G., Norris, R. N., Blusztajn, J. & Aubry, M. P. An osmium isotope excursion associated with the Late Paleocene thermal maximum: evidence of intensified chemical weathering. *Paleoceanography* **16,** 155–163 (2001).
46. Robert, C. & Kennett, J. P. Antarctic subtropical humid episode at the Paleocene–Eocene Boundary: clay-mineral evidence. *Geology* **22,** 211–214 (1994).
47. Goodwin, P. & Ridgwell, A. Ocean-atmosphere partitioning of anthropogenic carbon dioxide on multimillennial timescales. *Glob. Biogeochem. Cycles* **24,** GB2014 (2010).
48. Lord, N., Ridgwell, A., Thorne, M. & Lunt, D. An impulse response function for the "long tail" of excess atmospheric CO_2 in an Earth system model. *Glob. Biogeochem. Cycles* **30,** 2–17 (2015).
49. Palike, H. *et al.* A Cenozoic record of the equatorial Pacific carbonate compensation depth. *Nature* **488,** 609–614 (2012).

Acknowledgements

We thank the scientists and crew of IODP Expedition 342 and the IODP Bremen Core Repository. We thank M. Gilmour and S. Nicoara for assistance in the stable isotope laboratory at The Open University, V. Lukies for assistance in the XRF Core Scanning laboratory at MARUM, University of Bremen, and D. Andreasen for assistance with carbonate stable isotope analyses at the University of California, Santa Cruz. This work was supported by U.S. National Science Foundation Division of Ocean Sciences grant 1220615 to J.C.Z. and R.E.Z. and the Deutsche Forschungsgemeinschaft (DFG) (U.R. and T.W.).

Author contributions

D.E.P., S.K.T., P.F.S., R.D.N. and S.B. conceived the study and participated in IODP Expedition 342, which recovered and described the new sedimentary records. D.E.P. generated carbonate stable isotope analyses in the lab of J.C.Z. and A.J.D. generated organic carbon stable isotope and Coulormat wt% $CaCO_3$ analyses. XRF scanning records were generated by S.K.T. at Scripps and A.C., P.F.S., T.W. and U.R. at MARUM. D.E.P. and S.K.T. performed the carbon cycle modelling with guidance from R.E.Z. and A.R. D.E.P. wrote the manuscript with help from S.K.T. and P.F.S. All authors edited the manuscript.

Additional information

Supplementary information is available in the online version of the paper. Reprints and permissions information is available online at www.nature.com/reprints. Correspondence should be addressed to D.E.P.

Competing financial interests

The authors declare no competing financial interests.

Methods

Geochemical analyses. During IODP Expedition 342 (ref. 18), drilling operations penetrated the Palaeocene/Eocene (P/E) boundary at Site U1403 (39° 56.5997′ N, 51° 48.1998′ W, 4,946m depth) and Site U1409 (41° 17.7501′ N, 49° 13.9996′ W, 3,502m depth). Shipboard investigation described the lithology, identified the approximate position of the P/E boundary by nannofossil biostratigraphy and provided coarse-resolution records of the wt% of $CaCO_3$. The surfaces of the core archive halves spanning the PETM were scanned at 1–2 cm resolution at MARUM, University of Bremen, and at the Scripps Institution of Oceanography using Avaatech X-ray fluorescence (XRF) core scanners. Estimates of the total abundances of Ca and Fe were obtained by scanning the cores at an energy level of 10 kV, a current of 500 μA and a count time of 20 s with a measurement area of 10 × 12 mm. The estimated wt% $CaCO_3$ records were generated by regressing the shipboard wt% $CaCO_3$ measurements[18] against the natural logarithm of the XRF-derived Ca/Fe ratios. For stable isotope analyses, samples were collected at ~5 cm resolution from Site U1409 and 10 cm resolution from Site U1403, freeze-dried, homogenized with a mortar and pestle and analysed for $\delta^{13}C_{carb}$ in a ThermoFisher MAT 253 stable isotope mass spectrometer coupled to a Kiel IV carbonate device using standard dual-inlet techniques (the typical long-term $\delta^{13}C_{carb}$ reproducibility of the carbonate standards is <±0.05‰, 1 s.d.). In addition, samples from Site U1409 were washed and sieved and specimens of the benthic foraminifera *Nuttalides truempyi* were picked from the 150–212 and 212–300 μm size fraction. Where possible, 3–8 of these specimens from each sample were run using the $\delta^{13}C_{carb}$ methods described above. For $\delta^{13}C_{org}$ analysis of Site U1403 homogenized sample powders were decarbonated in 1 M HCl and washed with deionized water. $\delta^{13}C_{org}$ was measured using a Thermo-Finnegan MAT 253 mass spectrometer coupled to a Thermo Scientific 2000 HT elemental analyser via a Conflo IV interface optimized for the measurement of samples with low organic carbon abundances. Analytical reproducibility was monitored using analyses of International Atomic Energy Agency (IAEA) CH-6 sucrose and was <±0.1‰ (1 s.d.). All $\delta^{13}C$ data are expressed relative to the Vienna Pee Dee Belemnite standard. For Site U1403 the wt% $CaCO_3$ was measured using a Strohlein Coulormat.

Carbon cycle modelling. LOSCAR (Long-term Ocean Sediment CArbon Reservoir model) is a numerically efficient geochemical box model of the marine carbon cycle featuring realistic interactions with sediments and capable of multi-million year simulations of carbon cycle processes, including the CCD depth. All runs use the Palaeogene LOSCAR set-up[19]. cGENIE (Grid-ENabled Integrated Earth system model) is an intermediate-complexity Earth system model including a three-dimensional dynamic ocean model with biogeochemical cycling of key elements and isotopes and a spatially resolved sediment model that is capable of generating virtual sediment cores—synthetic stacks of deep-sea sediments[20,21,36]. We use the Late Palaeocene/Early Eocene configuration of ref. 37. For this study, we evaluate virtual sediment core results from a depth transect in the North Atlantic ranging from 5,000–3,000 m water depth and at locations that correspond to Expedition 342 sites.

Both models include carbonate and silicate weathering feedbacks. In LOSCAR weathering is parameterized as $F_w = F_{eq}([CO_2]_{atm}/[CO_2]_{eq})^{N_{Si}}$, where F_{eq} and $[CO_2]_{eq}$ are the equilibrium weathering flux and atmospheric p_{CO_2} at which volcanic carbon emissions are perfectly balanced by silicate weathering and carbonate burial[19]. N_{Si} sets the strength of the silicate weathering feedback (default $N_{Si} = 0.2$). We implement the same formulation for a CO_2-dependent carbonate and silicate weathering feedback in cGENIE using a model for terrestrial rock weathering[38]. Following ref. 39, we assume that carbonate weathering is proportional to the square root of $[CO_2]_{atm}/[CO_2]_{eq}$ and that silicate weathering is proportional to $[CO_2]_{atm}/[CO_2]_{eq}$ raised to the power of 0.3. We assume a 50/50 split between carbonate and silicate weathering to match the total carbonate burial, and to balance silicate weathering with volcanic outgassing. We used the cGENIE and LOSCAR models in this study to qualitatively demonstrate what mechanisms are consistent with the new data, not in an attempt to precisely reconstruct a PETM scenario.

Data availability. The stable isotope and XRF data that support the findings of this study are available from PANGEA at https://doi.org/10.1594/PANGAEA.860498.

Code availability. The C code for the LOSCAR model can be obtained on request from loscar.model@gmail.com. Instructions for obtaining the current version of cGENIE and a detailed description of the experiments used in this study are included in the Supplementary Information.